Articles

Electrogenicity of Electron and Proton Transfer at the Oxidizing Side of Photosystem II†

Michael Haumann, Armen Mulkidjanian, and Wolfgang Junge*

Abteilung Biophysik, FB Biologie/Chemie, Universität Osnabrück, D-49069 Osnabrück, Germany

Received December 19, 1996; Revised Manuscript Received May 15, 1997⊗

ABSTRACT: The electrogenicity of electron and proton transfer at the oxidizing side of PSII was monitored by transmembrane electrochromism of carotenoids in thylakoids and, independently, by electrometry in oxygen-evolving photosystem II core particles. It yielded dielectrically weighted distances between cofactors. They were related to the one between Y_Z^{ox} and Q_A^- (=100%). The electron transfer from Y_Z to P_{680}^+ ranged over a relative distance of 15%, while the one from Mn_4 to Y_Z^{ox} ranged over less than 3.5%. The latter result placed Mn_4 and Y_Z at about the same weighted depth in the membrane. The oxidation of cofactor X by Y_Z^{ox} during $S_2 \Rightarrow S_3$ ranged over 10%. We tentatively attributed 7% to proton transfer into the lumen and 3% to electron transfer, in line with our notion that one proton is liberated from X^{ox} itself. This placed X at the same depth in the membrane as Mn. Proton release upon the final oxidation of water during the oxygen-evolving step $S_4 \rightarrow S_0$ revealed relative electrogenic components of 5.5% in core particles and between 10.5% (pH 7.4) and 2% (pH 6.2) in thylakoids. The former likely reflected proton transfer from bound water into the lumen and the latter to intraprotein bases that were created in the foregoing transitions. A tentative scheme for the arrangement of cofactors at the oxidizing side of photosystem II is presented.

Photosystem II (PSII)[1] of green plants and cyanobacteria evolves oxygen at the expense of four quanta of light. The oxygen-evolving complex (OEC) contains a tetramanganese cluster (Debus, 1992; Brudvig, 1995). It is linked to the primary donor, P_{680}, by a redox-active tyrosine (D1Tyr161, Y_Z) (Barry, 1993, 1995; Britt, 1996). There is evidence that the OEC contains a further redox cofactor, named X in the following. Recent studies in our laboratory have shown that the cofactor X can be oxidized in chloride-depleted and in control PSII (Haumann et al., 1995, 1996; Hundelt et al., 1997). The optical difference spectrum of X^{ox} was similar to one that has been observed in calcium-depleted material and attributed to an oxidized histidine by Boussac et al. (1990). We therefore tentatively identified cofactor X with histidine (Haumann et al., 1996). Further studies have provided additional evidence for the oxidation of a histidine (Ono & Inoue, 1991; Allakhverdiev et al., 1992; Berthomieu & Boussac, 1995). In chloride-depleted material X^{ox} and Y_Z^{ox} were created on the first two redox transitions of the OEC (Haumann et al., 1996; Hundelt et al., 1997). In calcium-depleted material, however, the situation is less clear: X^{ox} [as identified by optical spectroscopy (Boussac et al 1990)] and Y_Z^{ox} [as identified by ENDOR (Tang et al., 1996)] may be observable at the same time. This may imply that these cofactors are in a redox equilibrium under certain conditions.

The OEC is located at the lumenal side of the thylakoid membrane. The three-dimensional structure of PSII is still lacking. The positions of the cofactors Mn_4, X, and Y_Z relative to the pigments of P_{680}, other chlorophyll molecules, pheophytins, and the quinone acceptors are not known. Structural models of PSII (Ruffle et al., 1992; Styring et al., 1993, Svensson et al., 1996) have been shaped in close analogy to the reaction center of purple bacteria (BRC). The structure of the primary donor of PSII, P_{680}, has been modeled in analogy to the BRC as an about parallel dimer of chlorophylls (Svensson et al., 1996). The degree of similarity between PSII and the BRC, however, is under debate because of their spectroscopic and electrochemical differences [Mulkidjanian et al., (1996) and references therein]. The functional studies of PSII, on the other hand, gave evidence that P_{680} may consist of two chlorophylls that are placed about perpendicular to each other (van Mieghem et al., 1991; Noguchi et al., 1993; Mulkidjanian et al., 1996). The location of the Mn cluster is unclear. It is conceivable that certain amino acids of the D1 and D2 proteins, of the extrinsic 33 kDa protein, CP47, and CP43 [see Nixon and

† Financial support by the Deutsche Forschungsgemeinschaft (SFB 171/A2), the Fonds der Chemischen Industrie, and from INTAS (INTAS-93-2852) is gratefully acknowledged. A.M. acknowledges additional funding by the Deutsche Forschungsgemeinschaft (Mu-1285/1-1 and Mu7-1285/1-2).

* Correspondence should be addressed to this author: Tel +49-541-9692872; Fax +49-541-9692262; e-mail JUNGE@UNI-OSNABRUECK.DE.

⊗ Abstract published in *Advance ACS Abstracts,* July 15, 1997.

[1] Abbreviations: BSA, bovine serum albumin; DCBQ, 2,5-dichloro-*p*-benzoquinone; DNP-INT, dinitrophenyl ether of iodonitrothymol; ENDOR, electron nuclear double resonance; EPR, electron paramagnetic resonance; FWHM, full width at half-maximum; Mes, 2-*N*-morpholinoethanesulfonic acid; Mn_4, the manganese cluster of PSII; P_{680}, primary donor; OEC, oxygen-evolving complex = Mn_4X entity; PSII, photosystem II; Q_A, primary quinone acceptor; S_i, *i*th oxidized state of the OEC; UV, ultraviolet; Y_Z, D1-tyrosine-161; X, chemically ill-characterized redox cofactor.

S0006-2960(96)03114-5 CCC: $14.00

Diner (1992), Pakrasi and Vermaas (1992), Vermaas et al. (1993), Barry et al. (1994), Pakrasi (1995), and Diner and Babcock (1996) for reviews] are involved in the creation of the protein environment of the OEC. An EPR triangulation based on radical signals from the non-heme iron and the tyrosine on D2, Y_D, yielded a central location of Mn between D1 and D2 at a large distance of about 20 Å from and below Y_Z (Un et al., 1994). A central location has also been inferred from electron microscopy of two-dimensional PSII crystals (Ford et al., 1995). Contrary to these results, model structures of PSII (Ruffle et al., 1992; Styring et al., 1993; Svensson et al., 1996) and our previous deconvolution of local electrochromic difference spectra (Cherepanov et al., 1995; Mulkidjanian et al., 1996) placed Mn_4 mostly on D1, out of the line that connects Y_Z and P_{680} and only slightly below Y_Z with respect to the membrane normal.

During the stepping of the catalytic cycle through the states S_0 to S_4, four electrons are successively withdrawn from the OEC. Two electron holes are likely stored on Mn during the transitions $S_0 \rightrightarrows S_1$ and $S_1 \rightrightarrows S_2$ (Klein et al., 1993). During $S_2 \rightrightarrows S_3$, the third hole is likely stored on a non-manganese component, X^{ox} (see above). Transition $S_3 \rightrightarrows S_4$ finally is coupled with the storage of the fourth hole on Y_Z (Bögershausen et al., 1996; Haumann et al., 1997). The state S_4 spontaneously decays into S_0 under release of dioxygen.

Protons are released into the lumen on every step of the catalytic cycle [see Lavergne and Junge (1993) and Haumann and Junge (1996) for reviews]. There are two types of proton release: (a) from peripheral amino acid residues that undergo a p*K* shift due to the electrostatic effect of a charge on Y_Z^{ox} and on the OEC (Haumann & Junge, 1994; Bögershausen & Junge, 1995) and (b) from redox cofactors and substrate water. Proton release of the latter type has only been detected during transition $S_2 \rightrightarrows S_3$, i.e., upon the oxidation of X (Haumann et al., 1995, 1996, 1997; Bögershausen et al., 1996; Hundelt et al., 1997), and on $S_4 \rightarrow S_0$ (Förster & Junge, 1985; Haumann & Junge, 1994).

The membrane separates two electrolyte phases and behaves as a capacitor. The light-induced transfer of one electron by PSII generates a transmembrane potential difference of about 25 mV [positive in the lumen, (Junge & Witt, 1968; Schliephake et al., 1968)], which is homogenized over almost all membranes in a chloroplast (Schönknecht et al., 1990). The membrane potential has been detected by an electrochromic shift of the absorption bands of carotenoids (Junge & Witt, 1968). The extent of the electrochromic transient is an intrinsic probe of the transfer of charges (protons and electrons) along the membrane normal. By monitoring electrochromism it has been shown that proton uptake upon the reduction of the non-heme iron in PSII is electrogenic (Haumann et al., 1995). Alternatively, the electrogenicity can be detected electrometrically by using macroscopic electrodes either with oriented membrane patches (Trissl & Gräber, 1980; Pokorny et al., 1994) or with vesicles that are attached to a planar bilayer (Drachev et al., 1981; Dracheva et al., 1987; Mamedov et al., 1995). Both approaches give insight into the directions, the dielectrically weighted relative distances, and the numbers of electrons and protons that are transfered over the respective native (thylakoid) or artificial (proteoliposome) membrane. The application of electrometric techniques to PSII has shown that electron transfer from Y_Z to P_{680}^+ spans a relative distance of between 13% and 18% relative to the distance between P_{680} and Q_A (Pokorny et al., 1994; Mamedov et al., 1995). The electron transfer from Q_A^- to Q_B contributes about 5% (Hook & Brzezinski, 1994; Mamedov et al., 1994). The electrogenicity of electron transfer from the OEC to Y_Z^{ox} has so far only indirectly been inferred from electroluminescence. For transition $S_2 \rightrightarrows S_3$ it was about 5% (Vos et al., 1991).

We studied the electrogenicity of electron and proton transfer in thylakoids and with PSII core particles during transitions $S_1 \rightrightarrows S_2$, $S_2 \rightrightarrows S_3$, and $S_3 \rightrightarrows S_4 \rightarrow S_0$. The half-rise times of electron transfer from Y_Z to P_{680}^+ in nanoseconds and from the OEC to Y_Z^{ox} in micro- to milliseconds were in parallel determined by flash photometry. By virtue of their kinetic properties, the electrogenic components were attributed to the various partial reactions of the OEC. The observed electrogenic components were deconvoluted into proton and electron transfer. On the basis of our and other data, we developed a model for the arrangement of the cofactors at the oxidizing side of PSII.

MATERIALS AND METHODS

Thylakoids (Jahns et al., 1991) *and O_2-evolving PSII core particles* [Bögershausen and Junge (1995); see also van Leeuwen et al., (1991)] were prepared as described previously and stored at −80 °C until use. Core particles were inactivated by incubating a suspension of 0.5 mM chlorophyll at pH 9 for 5 min. O_2 evolution in these samples was ≤10% of the controls [≈1200 μmol of O_2 (mg chlorophyll)$^{-1}$ h^{-1}].

Reconstitution of PSII Core Particles into Liposomes. Liposomes were prepared from asolectin from soybean (Sigma II). Asolectin (40 mg/mL) was dissolved in 10 mL of an ice-cold medium with 200 mM sucrose, 20 mM Tricine, pH 7.5, and 1.4% (w/v) sodium cholate. The solution was sonified on ice under argon (Branson sonifier, microtip output 4, 40% duty cycle) for 15 min to clearness and frozen in 1 mL portions at −80 °C until use. A Sephadex G25 column (NAP5, Pharmacia) was equilibrated with 10 mL of ice-cold buffer A (5 mM $CaCl_2$ and 2 mM Tricine, pH 7.5). Core particle stock (200 μL, about 0.5−0.8 mM chlorophyll) and 400 μL of liposomes were mixed, immediately loaded on the column, and eluted with 700 μL of buffer A. The middle fraction (400−500 μL) of the eluate was collected on ice and immediately used for the experiments.

Transmembrane electrochromism in thylakoids was recorded flash-spectrophotometrically (Junge, 1976) at 522 and 480 nm (Junge & Witt, 1968). After thawing, thylakoids were suspended in 10 mM NaCl, 10 μM DNP-INT, 2.6 g/L BSA, 2 mM hexacyanoferrate(III), and 100 μM DCBQ. With dark-adapted material (20 min, 40 μM chlorophyll) every transient was recorded on a fresh sample that was filled automatically into the cuvette (optical path length 1 cm) from a light-shielded reservoir. Under repetitive excitation the samples were excited by a train of flashes every 5 s. A Q-switched ruby laser (JK Lasers, 694 nm, FWHM 50 ns) provided the first flash of a train of saturating flashes and a xenon lamp (>610 nm, FWHM 10 μs) the following flashes. The flash-spacing was 500 ms. The use of the ruby laser avoided double hitting in the presence of the oxidized non-heme iron at the PSII acceptor side. Transients that where solely due to transmembrane electrochromism were obtained by subtracting the small background transients measured in

the presence of the potent ionophore gramicidin A (Sigma, 0.5 μM; Schönknecht et al., 1992) from the transients measured in the absence of gramicidin under otherwise unchanged conditions. The activity of PSI [monitored at 700 nm (Schaffernicht & Junge, 1982; not shown)] was less than 5% on the first flash and negligible from then on due to the presence of 200 μM DCBQ plus 2 mM hexacyanoferrate-(III) as electron acceptors.

Electron transfer at the OEC was monitored by UV transients at 360 nm as described previously (Renger & Hanssum, 1992; Bögershausen et al., 1996) and under similar conditions as in the measurements of electrochromism (see above).

Oxidoreduction of P_{680} was followed with nanosecond time resolution at 820 nm (see Figure 2) with a setup as in Haumann et al. (1996). A Nd−YAG laser (Qantel, 532 nm, FWHM 6 ns) served as excitation source.

As an alternative assay for the electrogenicity we used an electrometric technique that has been designed to detect charge transfer in proteoliposomes (Drachev et al., 1981). Reconstituted PSII core particles were attached to a lipid-impregnated nitrocellulose film. For further details and a sketch of the experimental setup see Drachev et al. (1979, 1981). The measuring cell consisted of two chambers (reference and sample) that were connected by a hole of 5 mm diameter, which was sealed by a thin collodion film. The film was prepared by spreading 30 μL of a solution of 1% (w/v) nitrocellulose (Agar Aids) in amyl acetate (Aldrich) on a water surface. Before being mounted into the measuring cell, the film was moistened with about 10 μL of 100 mg/mL asolectin in *n*-decane (Merck). Both chambers were filled with 4 mL of a medium with 400 mM sucrose, 400 mM betaine, 5 mM $CaCl_2$, 15 mM $MgCl_2$, and 20 mM Bis-Tris, pH 6.3. About 500 μL of a suspension of PSII containing liposomes were added to the sample chamber and gently stirred by a magnetic stirrer in darkness for 20 min. After this, the suspension in the sample chamber was replaced by fresh buffer (never dropping the medium surface below the collodion film) in order to remove unattached liposomes. Signals were detected by Ag/AgCl electrodes immersed in both cell chambers. The electrodes were freshly prepared before each experiment by covering a silver wire (0.5 mm diameter) with chloride in a bath of 1 M NaCl at a dc current of 5 mA for 1 h. In the cell chambers the electrodes were electrically connected to the solutions by agar bridges by placing them in a short black teflon tube and fixing with agar, 1.5% (w/v), and 3 M KCl. Voltage transients were amplified by an electrometer amplifier (electrical bandwidth dc to 10 MHz, gain 10, home-built) or an impedance converter (voltage follower, home-built) connected to a video amplifier (dc to 500 Mhz, gain 100, CLC100 Comlinear Corp.). The whole setup was placed in a HF-tight steel box. The figures show the extents of voltage transients before amplification. Transients were digitized by a Nicolet Pro92 recorder. Samples that contained proteoliposomes were repetitively excited (repetition period 30 s, Nd−YAG laser) by a train of nine flashes that were spaced by 100 ms [repetitive dark-adaption (Bögershausen & Junge, 1995)]. Under repetitive excitation the flash-train spacing was only 0.2 s.

Oxygen production under single flashes was recorded by a home-built centrifugable Clark-type electrode. Twenty microliters of a PSII-containing suspension was pelleted on its bare platinum surface by centrifugation (20 min in darkness, 20 °C, swing-out rotor, Beckmann TJ6 centrifuge, 3000 rpm). After connection of the electrode to a current-to-voltage amplifier (home-built) and 5 min of dark-adaptation, saturating xenon flashes (>610 nm, spacing 100 ms) were provided through a light guide and the resulting signals were digitized at 100 μs/address. The polarization voltage of −650 mV was applied to the platinum 2 min before the measurements.

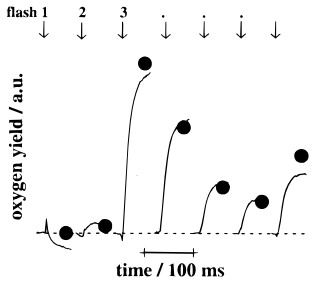

FIGURE 1: Transients of oxygen evolution from repetitively dark-adapted liposome-reconstituted PSII core particles as induced by a series of xenon flashes. Flash spacing 100 ms; 3 trains of 7 flashes were fired at 30 s intervals and averaged. Conditions: 50 μM DCBQ, 100 μM hexacyanoferrate(III) and 5 μM chlorophyll. The dots were calculated with Kok parameters of 21% misses, 2.9% double hits, and 100% of centers in state S_1 prior to the first flash.

RESULTS

(1) Properties of PSII Core Particles after Reconstitution in Liposomes. Figure 1 shows the extents of oxygen evolution induced by the first seven flashes given to repetitively dark-adapted, liposome-reconstituted PSII core particles (see Materials and Methods). The oxygen yield as function of the flash number oscillated with a period of 4. The data were fitted (Figure 1, dots) with the following set of Kok parameters: 21% misses (α), 3% double hits (β), and a relative population of S_1 of 100% in the dark. The oscillations proved that the core praticles were still active after the reconstitution procedure and similarly synchronized in the dark as untreated material (Haumann et al., 1994; Bögershausen & Junge, 1995).

Figure 2A shows electrometrically detected voltage transients on the first three flashes given to repetitively dark-adapted, liposome-reconstituted, O_2-evolving core particles under different electron acceptor conditions. Without external acceptor (−DCBQ, top), the first flash induced a large transient, and flashes 2 and 3 induced only small ones. A similar trace was observed with 1 mM hexacyanoferrate-(III) (not shown). With DCBQ as electron acceptor (+DCBQ, middle), similar transients were observed on flash 1 and on the following flashes. In inactive core particles (Figure 2A, bottom), the first transient was again similar as under the other conditions, but the ones on flashes 2 and 3 decayed more rapidly. We interpreted these results (Figure 2A) as follows: In the absence of an artificial electron acceptor, the first flash generated $S_2Q_A^-$. On the following flashes a stable charge separation was largely prevented because Q_A^- was still present. When DCBQ was added, Q_A^- decayed rapidly between flashes and the charge separation occurred on all flashes. That the first transient was still about 1.2 times larger than the following ones may be due to centers with slowed Q_A^- oxidation (Lavergne & Leci, 1993). In inactive centers a stable charge separation occured only on

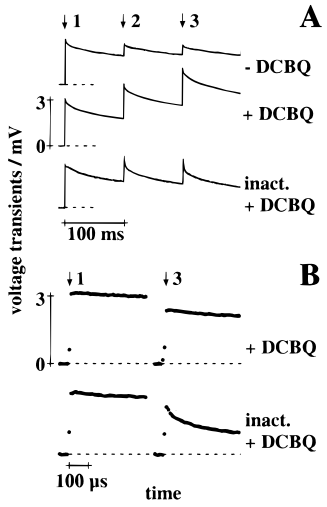

FIGURE 2: Flash-induced, electrometrically detected voltage transients in dark-adapted, liposome-reconstituted PSII core particles. (A) Transients on flashes 1−3 in the presence (top) and absence (middle) of 100 μM DCBQ. Bottom: inactive centers in the presence of DCBQ. Time resolution 50 μs/address, 10 transients averaged, xenon flashes every 100 ms. (B) Transients on flashes 1 and 3 in the presence of 100 μM DCBQ in control (+DCBQ, top) and centers that have been inactivated by pH 9 treatment (−DCBQ, inact., bottom) at a higher time resolution (10 μs/address) than in panel A. Thirty transients were averaged.

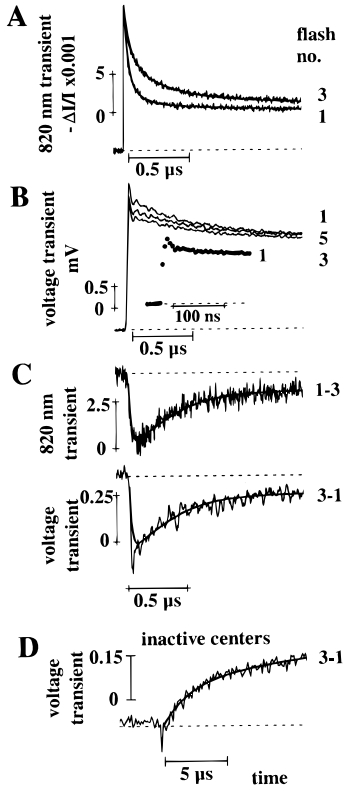

FIGURE 3: Comparison of the oxidoreduction of P_{680} monitored by optical spectroscopy and by voltage transients at nanosecond time resolution. (A) Absorption transients at 820 nm of repetitively dark-adapted PSII core particles on Nd−YAG flashes 1 and 3 (spacing 100 ms) indicating the oxidation (uprising) and reduction (decay) of P_{680}. Time resolution 4 ns/address; conditions 50 μM chlorophyll, 500 μM DCBQ, 1 mM hexacyanoferrate(III), 10 mM $CaCl_2$, and 20 mM Bis-Tris, pH 6.3. (B) Electrometrically detected voltage transients in dark-adapted, liposome-reconstituted PSII core particles on Nd−YAG flashes 1, 3, and 5 (spacing 100 ms). The extents were normalized on the first transient after 5 ms; for further conditions see Materials and Methods. Inset: the first flash on a 10-fold expanded time scale. Time resolution 5 ns/address; conditions 500 μM DCBQ and 1 mM hexacyanoferrate(III) as electron acceptors, 20 traces averaged on each flash. (C) Upper trace: difference of 820 nm transients on flashes 1−3 of the oxidoreduction of P_{680}^+ from panel A. Lower trace: the difference of electrometric voltage transients on flashes 3−1 from panel B. For the parameters of the calculated lines see text. (D) Difference of voltage transients from flashes 3−1 from centers that were inactive in oxygen evolution. Time resolution 50 ns/address; pH 7; transients from 10 series of three flashes given every 15 s were averaged.

flash 1 (see below). The polarity of the electrometric signals from core particles was opposite to the one obtained with chromatophores of *Rhodobacter capsulatus* (not documented). It implied that PSII was reconstituted into the liposomes with the donor side facing the outer surface of the membrane (inside-out), as in earlier work (Trissl & Gräber, 1980; Hook & Brzezinski, 1994; Mamedov et al., 1995). The inaccesibility of Q_A^- to hexacyanoferrate(III) corroborated this notion.

Figure 2B shows transients on flashes 1 and 3 in the control (top) and in inactive centers (bottom) at higher time resolution. The transients on the first flash were alike (see also Figure 2A, bottom). The one on flash 3 in inactive centers decayed with half-times of 40 and 260 μs (about 55% of the initial extent). With inactive centers, the first flash thus likely yielded Y_Z^{ox}/Q_A^- and the decays on the following flashes were attributable to recombination of the charge pair P_{680}^+/Q_A^- (Renger, 1979). In the control, charge recombination totaled only about 15% of the extent on the third flash. This result indicated that at least 80% of centers were still active in reducing Y_Z^{ox} by electrons from the OEC in the liposome-reconstituted material.

(2) Electrogenicity of the Electron Transfer from Y_Z to P_{680}^+ in Nanoseconds. Figure 3A shows absorption transients at 820 nm due to the oxidation (rise)/reduction (decay) of P_{680} on flashes 1 and 3, mainly inducing transitions $S_1 \Rightarrow S_2$ and $S_3 \Rightarrow S_4$ in repetitively dark-adapted core particles. The decays that reflect the electron transfer $Y_Z \rightarrow P_{680}^+$ were fitted with the following half-times and relative extents: first flash: 18 ns (44%), 70 ns (23%), 1.5 μs (23%), and a millisecond component of 10%; third flash, 35 ns (29%), 200 ns (32%), 1.75 μs (29%), and a millisecond component of again 10%. These half-times were similar to previously reported ones in the same type of core particle preparation (van Leeuwen et al., 1992).

Figure 3B depicts electrometric voltage transients induced by flashes 1, 3, and 5 in oxygen-evolving, repetitively dark-adapted, liposome-reconstituted core particles. The extents were normalized at 5 μs after the flash according to the following rationale: After 5 μs electron transfer from Y_Z to P_{680}^+ was completed and the state Y_Z^{ox}/P_{680} was reached in *all* centers whether active in oxygen evolution or inactive. The course of the transients between about 10 ns, e.g., after the formation of P_{680}^+/Q_A^- in the same centers, and 5 μs was therefore attributable to the electron transfer from Y_Z to P_{680}^+. The small spike on each trace (Figure 3B) resulted from the ringing of the amplifier. The transients rose with a half-time of $\leq$5 ns (see inset of Figure 3B for the first flash). It was probably limited by the duration of the laser flash (6 ns). It should be noted that without the agar bridges (see Materials and Methods) the time resolution was much lower, which had caused artifactual rising components in the 100 ns range [see also Trissl and Gräber (1980)]. The remaining transients decayed in nano- to milliseconds. The decay in the nanosecond time domain (Figure 3B) was more

Table 1: Electrogenicity of Reactions at the Oxidizing Side of PSII[a]

material	pH	electrogenicity, % of Y_Z^{OX}/Q_A^- formation (=100%)			
		$Y_Z \rightarrow P_{680}^+$	$S_1 \Rightarrow S_2$	$S_2 \Rightarrow S_3$	$S_4 \rightarrow S_0$
inactive core particles	6.5	8.0 ± 2 (2 μs)			
core particles	6.5	15.0 ± 4 (ns)	2.5 ± 1 (65 μs)	6.2 ± 1 (270 μs)	5.0 ± 1 (4.6 ms)
thylakoids	6.2	nd	nd	13.0 ± 3 (300 μs)	8.0 ± 3 (1.3 ms)[b]
	7.4	nd	4.0 ± 2 (60 μs)	13.0 ± 3 (220 μs)	16.5 ± 3 (1.2 ms)

[a] The kinetic components were detected by electrometry in core particles and by electrochromism in thylakoids. All extents are given as a percentage of the amplitude attributable to the formation of Y_Z^{ox}/Q_A^-. Figures in parentheses give the respective half-rise time of the reactions as determined from UV transients at 360 nm that were taken as a kinetic label for the electrogenic components. For the half-times of the reduction of P_{680}^+ in (nanoseconds), see text; nd, not determined. [b] This figure was tentatively obtained from the oscillation of the extents of electrochromism at 100 μs after flashes 1−8 in thylakoids (see Figure 8B).

rapid on flashes 1 and 5 than on flash 3. This variation of the decay time as a function of the flash number (Figure 3A) was interpreted as follows: On every flash the charge pair P_{680}^+/Q_A^- was formed in ≤1 ns (Trissl, 1989), which explained the initial rise. The electron transfer $Y_Z \rightarrow P_{680}^+$ (see above: Brettel et al., 1984; van Leeuwen et al., 1992) contributed further electrogenic components (Pokorny et al., 1994; Mamedov et al., 1995). The half-rise time of the latter was dependent on the flash number. Here, the expected rises were in part masked by decays, probably due to ionic leak currents. Figure 3C (upper trace) shows the difference of flashes 1−3 of the normalized transients at 820 nm from Figure 3A. It clearly reflected the slowing down of P_{680}^+ reduction on flash 3 (mainly transition $S_3 \Rightarrow S_4$) when compared with flash 1 ($S_1 \Rightarrow S_2$). The lower trace of Figure 3C reflects the difference of normalized voltage transients 3−1 from Figure 3B. It revealed the same slowing down on flash 3 as detected at 820 nm. This difference transient (Figure 3C, bottom) was well described under the assumption that electron transfer $Y_Z \rightarrow P_{680}^+$ on transitions $S_1 \Rightarrow S_2$ and $S_3 \Rightarrow S_4$ contributed an electrogenic component of 15% (Table 1) relative magnitude as compared with the one attributed to P_{680}^+/Q_A^- formation. The line in Figure 3C (bottom) was calculated with the same half-times as the electron transfer $Y_Z \rightarrow P_{680}^+$ as obtained from the transients at 820 nm in Figure 3A. As there may be a portion of centers that was inhibited due to acceptor side lesion after flash number one (compare Figure 2), we consider an extent of the electrogenicity of 15% for $Y_Z \rightarrow P_{680}^+$ as the lower limit.

With centers that were inactive in oxygen evolution (see Materials and Methods) the difference of voltage transients from flashes 3−1 (Figure 3D) revealed an additional rising electrogenic component on flash 1 with a half-rise time of about 2 μs and relative extent of about 8% of the formation of P_{680}^+/Q_A^- (Table 1). The half-rise time was typical for electron transfer from Y_Z to P_{680}^+ in inactive centers at pH 7 (Conjeaud & Mathis, 1980). The electrogenic extent (Figure 3D), however, was smaller than for the same reaction in oxygen-evolving material. This result may indicate a more hydrophilic environment of Y_Z in inactive centers. The same effect may account for its increased accessibility to external reductants (Yerkes et al., 1983).

(3) Electrogenic Reactions of the Oxygen-Evolving Complex: (a) Liposome-Reconstituted PSII Core Particles—electrometry. The rates of electron transfer at the OEC were determined from UV-transients at 360 nm which reflect redox changes of the OEC (Renger & Hanssum, 1992). Figure 4A shows raw transients on flashes 1, 2, and 3 given to repetitively dark-adapted PSII core particles. Each flash induced a rapid jump mainly due to the formation of Q_A^-

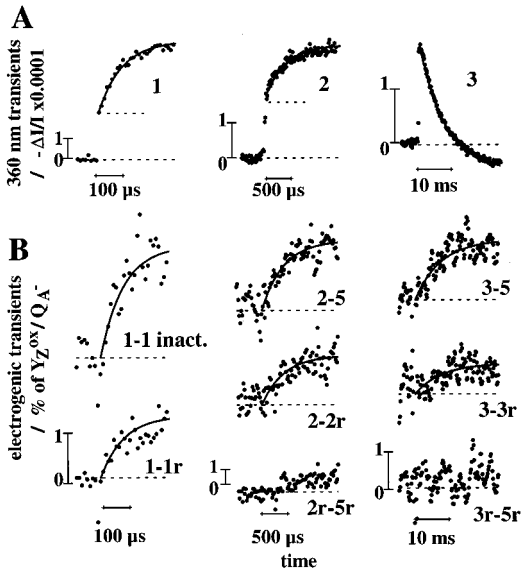

FIGURE 4: UV transients and voltage transients upon oxidoreduction of the OEC at higher time resolution in dark-adapted core particles. (A) Absorption transients at 360 nm due to xenon flashes 1, 2, and 3 (from left to right). Conditions: 8 μM chlorophyll, 200 μM DCBQ, 10 mM $CaCl_2$, and 10 mM Mes, pH 6.5. xenon flashes every 100 ms; 20 series of flashes at 30 s spacing were averaged; time resolution 10 μs/address. (B) Differences of electrometrically detected voltage transients from repetitively dark-adapted, liposome-reconstituted core particles. The extents are given as a percentage of the one attributable to the formation of Y_Z^{ox}/Q_A^- (for further conditions see Materials and Methods). 1 − 1 inact., flash 1 from oxygen-evolving material minus flash 1 from pH 9 treated material; all other traces, oxygen-evolving material; 1 − 1r (2 − 2r, 3 − 3r): flash 1 (2, 3) from dark-adapted minus flash 1 (2, 3) from repetitive excitation; 2 − 5 (3 − 5), flashes 2 (3) minus 5 from dark-adapted material; 2r−5r (3r−5r), flash 2 (3) minus 5 from repetitive excitation. Note the different time scales in panel B. Up to 10 transients were averaged per flash at a time resolution of 10 μs (flashes 1 and 2) or 100 μs (flash 3) per address. For the parameters of the calculated lines see text.

(dashes). The jump was followed by slower rises on flashes 1 and 2, which were mainly attributable to the oxidation of Mn on transition $S_1 \Rightarrow S_2$ (flash 1) and of the cofactor X [probably histidine (Haumann et al., 1996)] on $S_2 \Rightarrow S_3$ (flash 2) by Y_Z^{ox}. The half-rise times were 65 and 270 μs, respectively (Figure 4A, Table 1). The decay on the third flash (Figure 4A, right trace) was attributed to the reduction of the OEC by electrons from bound water during transition $S_4 \rightarrow S_0$. Its half-decay time was 4.6 ms, similar to a figure found previously in this type of material (van Leeuwen et al., 1993).

Voltage transients due to a series of eight flashes were recorded electrometrically with repetitively dark-adapted core particles that were reconstituted into liposomes (data not

shown but see Figure 2A, middle, for some raw transients). On a micro- to millisecond time scale the transients revealed, on a first glance, only decays (compare Figure 2). Electrogenic components were attributed to the partial reactions of the OEC as characterized by the above-determined half-times of electron transfer (Table 1). We compared three different sets of data: (i) the difference of transients from dark-adapted oxygen-evolving material minus transients from centers that were inactivated by pH 9 treatment (see Materials and Methods), (ii) the difference (after amplitude normalization) of transients obtained with repetitively dark-adapted material minus transients from repetitive flash excitation, and (iii) the difference of transients on different flashes out of the *same* flash series from dark-adapted material. The difference of transients from dark-adapted minus repetitively excited material canceled all components unrelated to the turnover of the OEC. The cancellation resulted because in the former material the centers were synchronized in S_1 prior to flash 1 whereas in the latter the four S transitions contributed about equally on each flash. Differences of transients from the same series were taken because then the individual S transitions contributed differently on each flash.

The left column of Figure 4B shows the differences of transients from dark-adapted oxygen-evolving core particles minus inactive material (top, 1 − 1 inact.) and from dark-adapted oxygen-evolving material minus repetitive excitation (bottom, 1 − 1r) on flash 1 (mainly $S_1 \Rightarrow S_2$) (the time bars are the same for all traces in one column). Both differences revealed additional electrogenic rise components on the first flash in dark-adapted active material. These components were absent in both inactive and repetitively excited centers. The extents of these transients were 2.1 and 1.3% of the one attributable to formation of the charge pair Y_Z^{ox}/Q_A^- in active material (e.g., 10 μs after the exciting flash; compare Figure 2B). The electrogenic rises were well described with the half-time of 65 μs (Figure 4B, left, straight lines) as obtained from the respective UV transient.

We compared transients on flash 2, mainly inducing $S_2 \Rightarrow S_3$, with those on flash 5. The latter mainly induced $S_1 \Rightarrow S_2$, similar to flash 1 but without contributions from the non-heme iron (Haumann et al., 1995). The differences of transients on flashes 2 minus 5 from dark-adapted centers (Figure 2B, middle column, top trace, 2 − 5) and of flash 2 from dark-adapted centers minus flash 2 from repetitive excitation (middle trace, 2 − 2r) revealed kinetic components with extents of 4% and 3% of Y_Z^{ox}/Q_A^- formation. These electrogenic rises were described with a half-time of 270 μs (straight lines), again derived from the UV measurements. As a control, the difference of transients 2 minus 5 from repetitive excitation was taken (Figure 4B, middle column, bottom, 2r − 5r). This difference was close to zero, as expected for an about equal contribution of all S transitions on both flashes (see also Figure 5 and below).

Was there a kinetic component with the characteristic half-time of $S_4 \rightarrow S_0$ on flash 3? The differences of transients 3 minus 5 from dark-adapted material (Figure 4B, right column, top, 3 − 5) and transients 3 dark-adapted minus 3 repetitive (middle, 3 − 3r) revealed additional rises on flash 3 with extents of 1.8% and 1.2% of Y_Z^{ox}/Q_A^- formation and a half-time of 4.6 ms (straight lines). The difference between transients 3 minus 5 from repetitive excitation (bottom, 3r − 5r) was about zero, again in accordance with an about equal contribution of all S transitions on each flash.

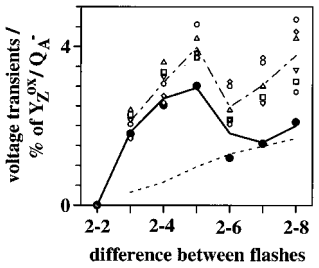

FIGURE 5: Extents of the difference of voltage transients 2 − 2 to 2 − 8 (as in Figure 4B) from liposome-reconstituted core particles. The extents are given as a percentage of the one attributable to Y_Z^{ox}/Q_A^- formation. Open symbols: Data from 6 individual experiments with dark-adapted material; the dashed-dotted line connects the average points. Dotted line: Differences of flashes 2 − 2 to 2 − 8 from repetitively excited material (one train of flashes every 0.2 s). Solid circles: Differences of the average extents from dark-adapted minus the ones from repetitively excited material. The solid line was calculated with Kok parameters as listed in the text.

We deconvoluted the raw extents of the electrogenic components (Figure 4B) into the ones attributable to the pure S transitions. Figure 5 shows the extents of the differences of flashes 2 minus 3−8 of dark-adapted material from six individual experiments (open symbols). The average over all experiments revealed a clear quarternary oscillation (dashed-dotted line). On the differences of flash 2 minus 3−8 from repetitive excitation, this oscillation was absent (dotted line). Small nonoscillating components were, however, also observed in this case. They were attributed to the increase in the amount of inactive centers that underwent charge recombination between P_{680}^+ and Q_A^- with increasing flash number ($\leq$20%). The latter extents were subtracted from the ones from dark-adapted material. The resulting extents (Figure 5, ●) were well described (solid line) with a set of Kok parameters of 21% misses, 3% double hits, and 100% of centers initially in state S_1 as determined from oxygen evolution (see above). We assumed that a rising electrogenic component with 5.2% extent of Y_Z^{ox}/Q_A^- formation and $t_{1/2}$ of 270 μs was only present on transition $S_2 \Rightarrow S_3$. The ratio of the extents of the 270 μs components on the differences 2 − 5/2 − 2r (Figure 4B, middle) was 1.3. This figure matched the one that was expected on the basis of the above Kok parameters. These results strongly corroborated the notion that the liposome-reconstituted centers were similarly synchronized in the dark as their counterparts in solution. With an amount of about 20% of inactive centers in the former material, the 270 μs component on transition $S_2 \Rightarrow S_3$ was recalculated to yield an electrogenicity of 6.2% (Table 1) of Y_Z^{ox}/Q_A^- formation.

How large was the 65 μs component that was detected on the first flash, which induced mainly $S_1 \Rightarrow S_2$? The extent of the difference of flashes 1 − 1 inact. (Figure 4B) of 2.1% was recalculated to 2.5% under the assumption of 21% misses (see above). That the difference 1 − 1r (Figure 4B) was smaller, 1.3%, was compatible with the expectation of a 25% contribution of all S transitions under repetitive excitation and a miss parameter of again 21% on the first flash ($S_1 \Rightarrow S_2$) in dark-adapted material. The latter result indicated that if a small contribution of transition $S_0 \Rightarrow S_1$ was still present on the first flash, it was well below 1%.

On the third flash (mainly $S_4 \rightarrow S_0$), the 4.6 ms component of 1.8% on the difference 3 − 5 (Figure 4B) was recalculated with the above Kok parameters and an amount of 20% of inactive centers to yield a true extent of 5% (Table 1) of

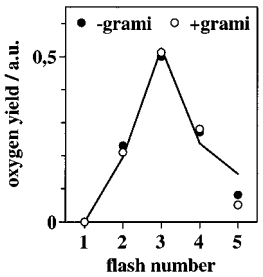

FIGURE 6: Oxygen yields of the first five flashes in dark-adapted thylakoids in the presence (○) and absence (●) of 0.5 μM gramicidin A. Conditions: xenon flashes every 100 ms; 20 μM chlorophyll, pH 7.4. The line was calculated with the Kok triple given in the text.

Y_Z^{ox}/Q_A^-. The raw extent of the difference 3 − 3r (Figure 4B) of 1.2% was close to the one of 1.4% that was expected on the basis of the above parameters and a 25% contribution of all S transitions under repetitive excitation. The amplitudes of the electrogenic components on transitions $S_1 \Rightarrow S_2$, $S_2 \Rightarrow S_3$, and $S_4 \rightarrow S_0$ are again summarized in Table 1.

In the above analysis, possible electrogenic contributions of transition $S_0 \Rightarrow S_1$ were neglected: According to our data (Bögerhausen et al., 1996; Haumann et al., 1997), electron transfer from Mn_4 to Y_Z^{ox} proceeds with a much smaller half-rise time of about 50 μs than the ones of both $S_2 \Rightarrow S_3$ (220 μs) and $S_4 \rightarrow S_0$ (4.6 ms) in the type of core particles used. Furthermore, the first flash did only induce transition $S_1 \Rightarrow S_2$ due to a 100% population of S_1 in the dark (see above). We conclude that components from $S_0 \Rightarrow S_1$ were not included to a significant extent (less than 1%) in the electrogenic components that occurred with the half-rise times of the other transitions.

(b) Thylakoids—Transmembrane Electrochromism of Carotenoids. Figure 6 shows the oxygen yields on the first five flashes from dark-adapted thylakoids in the presence (○) and absence (●) of gramicidin. The quarternary oscillations of oxygen evolution were alike in both cases. This behavior indicated a similar stepping of the OEC through the S states under both conditions. The pattern was described with Kok parameters of 10% misses, 14%, double hits, and 15% and 85% of centers in states S_0 and S_1 in the dark (at pH 7.4, Figure 6, line). At pH 6.2 a similar experiment (not shown) yielded a higher portion of S_1, 100%, as previously found (Haumann & Junge, 1994).

UV transients at 360 nm which were attributable to the oxidoreduction of the OEC were measured in dark-adapted thylakoids. Figure 7A shows the transients induced by flash 2, mainly inducing transition $S_2 \Rightarrow S_3$ (left), and by flash 3, mainly inducing $S_3 \Rightarrow S_4 \rightarrow S_0$ (right), at pH 7.4. The half-rise time of the slower rising component on top of the jump on flash 2 was 220 μs (Table 1). This component was attributable to the oxidation of X on $S_2 \Rightarrow S_3$ (Bögershausen et al., 1996). The decay on the third flash indicated the reduction of the OEC by electrons from water on $S_4 \rightarrow S_0$. Its half-decay time was 1.2 ms (Table 1).

Electrochromic absorption transients were measured as function of the flash number at 522 nm. The small background at this wavelength was obtained separately in the presence of 0.5 μM gramicidin and subtracted. To resolve electrochromic components that were correlated with the turnover of the OEC, we again took the differences of transients as obtained on different flashes with dark-adapted

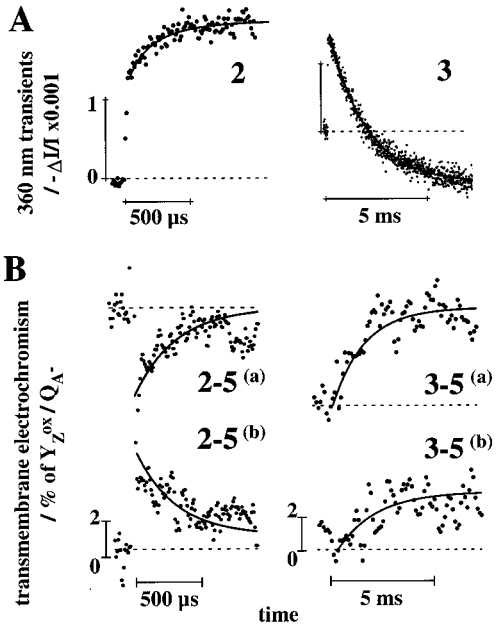

FIGURE 7: UV transients at 360 nm and transmembrane electrochromic absorption transients in dark-adapted thylakoids. (A) UV transients at 360 nm on flashes 2 and 3: 30 μM chlorophyll; 100 transients averaged; xenon flashes every 100 ms; 200 μM DCBQ and 1 mM hexacyanoferrate(III) (B) Electrochromic absorption transients at 522 nm. For the conditions see Materials and Methods. All differences were obtained from transients which represented the difference ± 500 nM gramicidin; the pH was 7.4. Left column: differences of transients on flashes 2−5 from dark-adapted material; trace a, at 522 nm; trace b, at 480 nm. Right column: differences of transients at 522 nm on flashes 3−5; trace a, pH 7.4; b, pH 6.2. The time resolution was 10 μs (differences 2 − 5, 300 transients averaged, amplitude normalized at 2 ms after the flash) or 100 μs (differences 3 − 5, 200 transients averaged, extent normalized at 100 μs after the flash). For the parameters of the lines see text.

material (compare Figure 4). Figure 7B shows the resulting difference transients. The difference of flashes 2 minus 5 at a wavelength of 522 nm (after normalization of the respective amplitudes after 2 ms, left, trace a) revealed a rising component on flash 2, which was described with the same half-time of 220 μs (line) as obtained from the UV transient on the second flash (see above). Its electrogenic extent was about 5.6% of the one attributable to the formation of Y_Z^{ox}/Q_A^-. When this experiment was carried out at 480 nm, a transient with the same half-rise time (220 μs) and similar extent (6.5%) but with inverted sign was observed (Figure 7B, left, trace b). The sign inversion was expected if the kinetic components were due to carotenoid bandshifts (Schliephake et al., 1968). The half-rise time of 220 μs was typical for electron transfer on transition $S_2 \Rightarrow S_3$ [see (Haumann et al. (1996) and above]. The same experiment carried out at pH 6.2 (data not shown) revealed (at 522 nm) a component with a half-rise time of 300 μs and an extent of 6.5% on the difference of flashes 2 minus 5. The extents of the electrogenic components were scaled according to the above Kok parameters. This yielded 13% (Table 1) as the true electrogenicity on $S_2 \Rightarrow S_3$. A similar figure of 12% has been previously obtained in experiments with chloride-depleted thylakoids (Haumann et al., 1995).

That there was an electrogenic rising component on transition $S_4 \rightarrow S_0$ which oscillated in a series of flashes was already evident from an inspection of the electrochromic transients at 522 nm after normalization of their amplitudes

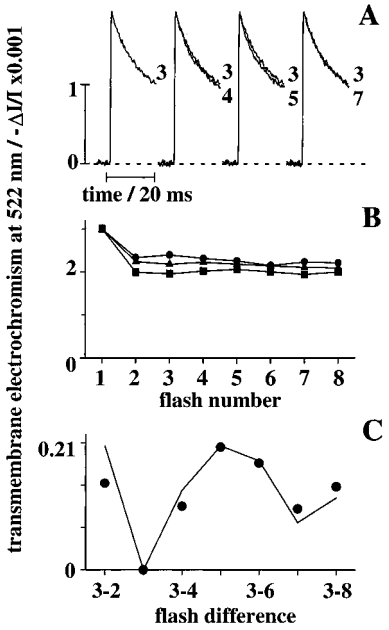

FIGURE 8: Electrogenic reactions on transition $S_4 \rightarrow S_0$. (A) Electrochromic absorption transients on flashes 3, 4, 5, and 7 in dark-adapted thylakoids. The amplitudes were normalized on flash 3 for comparison. The time resolution was 100 μs/address, and 200 transients were averaged. (B) Extents of 522 nm transients at 100 μs (■), 1.5 ms (▲) and 10 ms (●) after the respective flash as function of the flash number. The extents were normalized in order to make them equal on the first flash after all time intervalls. This procedure compensated for the flash number-independent relaxation of all transients due to ionic leak currents. (C) The extents (dots) of the difference of transients on flashes 3 − 2 to 3 − 8 oscillated with period of 4. The line was calculated with the Kok parameters given in the text.

at 100 μs. Transients on flashes 4, 5, and 7 are compared with flash 3 in Figure 8A. The transient on flash 5 decayed faster than the one on flash 3. On transient 7 (which was flash 3 of the second cycle of the OEC) the difference was again smaller.

The right part of Figure 7B shows the differences of electrochromic transients at 522 nm on flashes 3 minus 5 at pH 7.4 (after amplitude normalization at 100 μs, top, trace a) and 6.2 (bottom, trace b). These differences revealed additional electrogenic rising components on flash 3, which were described (lines) with half-times of 1.2 ms and extent of 6% of the formation of Y_Z^{ox}/Q_A^- at pH 7.4 and of 1.3 ms and 3.5% at pH 6.2. These half-times were similar to the ones on $S_4 \rightarrow S_0$ from the UV transients. In a similar experiment but under repetitive flash excitation (not shown), the difference of flashes 3 minus 5 was negligible, as expected for an about equal contribution of all S transitions on each flash.

We deconvoluted the extents of the millisecond component on flash 3 with the above Kok parameters. At pH 7.4, about 56% and 11% of centers underwent transition $S_4 \rightarrow S_0$ on flashes 3 and 5, and at pH 6.2, 56% and 10%. Thus, the millisecond components on the differences 3 − 5 were scaled up by factors of 2.2 and 1.65 to yield the true extents of the electrogenic rises of 13% and 6% on $S_4 \rightarrow S_0$.

As an independent approach to estimate the extent of electrogenicity on transition $S_4 \rightarrow S_0$, we plotted the extents of electrochromic transients (Figure 8B) at times of 100 μs (■), 1.5 ms (▲) and 10 ms (●) after the respective flash. The amplitudes were normalized according to the first flash to compensate for the flash number-independent decay of the raw electrochromic transients (see Figure 8A) due to transmembrane ionic leak currents. Already after 100 μs (Figure 8B, ■) the extents on flashes 2−8 showed a quarternary oscillation with minima on flashes 3 and 7, which mainly induce $S_3 \Rightarrow S_4 \rightarrow S_0$. This oscillation in part reflected the electrogenicity of the reduction of P_{680}^+ by Y_Z [see section 2 under Discussion and Schlodder et al., (1985) and Rappaport et al., (1995)]. A further source was likely the electron transfer OEC $\rightarrow Y_Z^{ox}$. It was about completed after 100 μs only on transitions $S_0 \Rightarrow S_1$ and $S_1 \Rightarrow S_2$. From the data in Figure 8B we calculated the extent of the latter to be about 4% of Y_Z^{ox}/Q_A^- formation. The extents at 10 ms after the respective flash showed a similar oscillation (Figure 8B, ●) but with *maxima* on flashes 3 and 7. This behavior revealed that the rising electrogenic component associated with transition $S_4 \rightarrow S_0$ was larger than on the other transitions (at pH 7.4).

The extents of the differences on flashes 3 minus 2−8 (at 10 ms) are shown in Figure 8C (dots). The oscillations of these extents were described with similar Kok parameters as determined above and under the assumption that an electrogenic component with an extent of 20% of the one attributable to Y_Z^{ox}/Q_A^- formation was only present on $S_4 \rightarrow S_0$ (line in Figure 8C). A similar experiment at pH 6.2 yielded an extent of 10% (not documented). These extents were somewhat larger than in the determination from transients with amplitude normalization at 100 μs. The average extents of the electrogenic rises on $S_4 \rightarrow S_0$ were thus 16.5% and 8% of Y_Z^{ox}/Q_A^- formation at pH 7.4 and 6.2. They are summarized in Table 1.

DISCUSSION

(1) Electrogenicity of Electron Transfer from Y_Z to P_{680}^+. The lower limit of the electrogenicity of the reduction of P_{680}^+ by Y_Z in liposome-reconstituted, O_2-evolving PSII core particles was 15% of the one of Y_Z^{ox}/Q_A^-. It was in the range that has previously been determined for BBY membranes from pea (Pokorny et al., 1994) and core particles from Synechococcus (Mamedov et al., 1995). Assuming a distance between P_{680} and Q_A of 23 Å (Mulkidjanian et al., 1996) and a homogenous dielectric, the projection of the position of Y_Z (i.e., of the positive charge center on the tyrosine entity) on the membrane normal was at about 3.5 Å below the position of P_{680} (i.e., of the positive charge center on P_{680}). This position is compatible with a placement of Y_Z on subunit D1 and at a position occupied by LArg135 in the bacterial reaction center (Michel & Deisenhofer, 1988). A similar conclusion has been reached on the basis of an analysis of local electrochromic bandshifts in the red spectral region (Mulkidjanian et al., 1996). The extent of the electrogenicity was about halved in centers that were inactivated in oxygen evolution. Instead of attributing the diminution to a decay of distances, we tend to assume that the removal of Mn from its binding pocket doubled the dielectric permittivitiy (through access of water) around Y_Z.

(2) Comparison of Electrogenic Components in Thylakoids and Core Particles. The electrogenicity of electron transfer from Y_Z to P_{680}^+ was the same when determined in BBY membranes (Pokorny et al., 1994) and core particles (Mamedov et al., 1995; this work). These results indicated that the dielectric permittivity between these cofactors was

Table 2: Electrogenicities of Proton Transfer at the Oxidizing Side of PSII[a]

		electrogenicity of proton transfer, % of Y_Z^{OX}/Q_A^- formation (=100%)		
material	pH	$S_1 \Rightarrow S_2$	$S_2 \Rightarrow S_3$	$S_4 \rightarrow S_0$
core particles	6.5	(3.4)[b]		5.5 (6.5)[b]
thylakoids	6.2	≤ 3.5[c] (5.1)[b]	6.5 (6.5)[b]	2.0 (4.0)[b]
	7.4	(1.7)[b]		10.5 (9.0)[b]

[a] Electron transfer OEC → Y_Z^{ox} was assumed to contribute ≤ 3.5% of Y_Z^{ox}/Q_A^- formation. The other electrogenicities are therefore lower estimates. All figures were corrected for the extents that were attributable to the electrogenic reduction of P_{680}^+ in microseconds (see Discussion). [b] The figures in parentheses are theoretical figures calculated according to the geometry shown in Chart 1. The values in core particles were tentatively normalized by a factor of 2 at the same dielectric permittivity as in thylakoids (see text). [c] The figure of ≤ 3.5% on $S_1 \Rightarrow S_2$ is the upper estimate.

independent of the preparation. On the contrary, the electrogenicity of electron transfer on transitions $S_1 \Rightarrow S_2$ and $S_2 \Rightarrow S_3$ was about halved in core particles when compared with thylakoids (Table 1). This is likely attributable to an increased dielectric permittivity around Mn_4 and X in core particles, perhaps owing to the absence of the extrinsic 17 and 23 kDa proteins (van Leeuwen et al., 1991). For the comparison of the electrogenic reactions at the OEC we tentatively scaled up the extents from core particles by the same relative dielectric permittivity of thylakoids, by a factor of 2 (see Table 1).

(3) Electrogenic Reactions at the OEC: Deconvolution into Electron and Proton Transfer. To unravel the electrogenicity attributable to electron transfer from Mn and X to Y_Z, we used the characteristic time constants of these events during transitions $S_1 \Rightarrow S_2$, $S_2 \Rightarrow S_3$, and $S_4 \rightarrow S_0$. The raw electrogenicities had to be corrected for the electrogenic contributions that resulted from the redox equilibrium between P_{680} and Y_Z. The proportion of P_{680}^+ is about 10% in states S_0 and S_1 and larger, about 20%, in the more oxidized states S_2 and S_3 (Schlodder et al., 1985; Rappaport et al., 1995). The electron transfer $Y_Z \rightarrow P_{680}^+$ was electrogenic with about 15% of P_{680}^+/Q_A^- formation. Thus, we expected an electrogenic contribution of 1.5% on transition $S_1 \Rightarrow S_2$ from the electron transfer between Y_Z and P_{680}^+ when an electron from the OEC was transferred to Y_Z^{ox} and further on to P_{680}^+. By subtraction of the figure of 1.5% due to the electron transfer between Y_Z and P_{680}^+ from the raw figure of 5% on $S_1 \Rightarrow S_2$ (Table 1), the electrogenic component of electron transfer from Mn_4 to Y_Z^{ox} on $S_1 \Rightarrow S_2$ was recalculated to 3.5%. On $S_1 \Rightarrow S_2$ the electrogenicity of proton release was probably small as it occurred only from peripheral amino acid groups [see Haumann and Junge (1996) for a review]. Accordingly, 3.5% was the upper limit of the electrogenicity of electron transfer from Mn_4 to Y_Z^{ox} (Table 2).

That the above electrogenicity on transition $S_1 \Rightarrow S_2$ was small corroborated our previous data from chloride-depleted thylakoids (Haumann et al., 1995; Hundelt et al., 1997): There, the electrogenicity on transition $S_1 \Rightarrow S_2$ in controls was smaller than upon the oxidation of X on transitions $S_1^* \Rightarrow S_2^*$ in chloride-depleted centers and on $S_2 \Rightarrow S_3$ in controls (Haumann et al., 1995; Hundelt et al., 1997). These and the above data indicate that the oxidation of manganese on transition $S_1 \Rightarrow S_2$ was less electrogenic than the events coupled to the oxidation of X on $S_2 \Rightarrow S_3$.

In the higher oxidation states the equilibrium proportion of $Y_ZP_{680}^+$ was about 20% (see above). On this basis, electrogenic components with microsecond half-times and with relative extents of about 3% were expected on transitions $S_2 \Rightarrow S_3$ and $S_4 \rightarrow S_0$. They originated from electron transfer $Y_Z \rightarrow P_{680}^+$. The observed electrogenic components after these transitions, however, were much larger (Table 1) and thus coupled to the turnover of the OEC. We corrected the raw electrogenicities on transitions $S_2 \Rightarrow S_3$ and $S_4 \rightarrow S_0$ by subtracting the 3% as attributable to electron transfer $Y_Z \rightarrow P_{680}^+$.

Were the resulting electrogenic components (Table 2) attributable to electron transfer or to proton release? The electrogenicity of the electron transfer from Mn to Y_Z^{ox} was estimated to be small (less than 3.5%, see above). Water is probably bound to Mn atoms. Thus, it is reasonable to assume that most of the electrogenicity observed on transition $S_4 \rightarrow S_0$ is attributable to proton transfer from the water molecules that are bound at about the same level in the membrane as Mn into the aqueous phase at the lumen side (see Table 2). On transition $S_2 \Rightarrow S_3$, cofactor X is likely oxidized. We cannot exclude the possibility that X is placed at a level below Mn in the membrane. However, we consider it as more likely that the electrogenicity of electron abstraction from X is about the same as upon the oxidation of Mn. We therefore attributed most of the electrogenicity observed on transition $S_2 \Rightarrow S_3$ to proton transfer from X^{ox} to the lumen.

This view was corroborated by the following observation: The pH dependence of the extents of these electrogenic reactions paralleled the one that has been observed in direct measurements of the extent of proton release in these preparations on transitions $S_2 \Rightarrow S_3$ and $S_4 \rightarrow S_0$:

On transition $S_2 \Rightarrow S_3$, one proton was released independent of the pH (Haumann & Junge, 1996). We have shown by comparison of proton release from chloride-depleted and control PSII that this proton likely results from the oxidation of the cofactor X (Haumann et al., 1996; Hundelt et al., 1997). This conclusion was based on the observations of a much larger H/D isotope effect and a greater activation energy of electron transfer from X to Y_Z^{ox} on $S_2 \Rightarrow S_3$ in controls and on $S_1^* \Rightarrow S_2^*$ in chloride-depleted centers (Haumann et al., 1997; Bögershausen et al., 1996; Hundelt et al., 1997). In line with the observation of a pH-independent release of one proton on $S_2 \Rightarrow S_3$, the electrogenicity on this transition was independent of the pH. The extent of the electrogenicity of the transfer of one proton to the lumen was here calculated as 6.5% of the one of Y_Z^{ox}/Q_A^- formation (Table 2). This figure was similar to the one that we estimated in chloride-depleted thylakoids (Haumann et al., 1995; Hundelt et al., 1997). We summarize our proposed reactions on transition $S_2 \Rightarrow S_3$ in Scheme 1A.

On $S_4 \rightarrow S_0$, the electrogenicity that was attributable to proton transfer was variable (Table 2). It increased from thylakoids at pH 6.2, over core particles (pH 6.5) to thylakoids at pH 7.4 (Table 2). The extent of proton release as monitored with pH-indicating dyes reveals the same strong pH dependence (Haumann & Junge, 1994): It ranges from 1.7 protons at pH 7.4 over 1 at about pH 6.5 to 0.3 at pH 6.1 in thylakoids. This variability has been explained by the following rationale: In state S_4, three protons are still present in the center [two from one bound water molecule and one from the OH^- molecule probably bound on transition

Scheme 1: Electrogenicities of Electron and Proton Transfer at the Oxidizing Side of PSII[a]

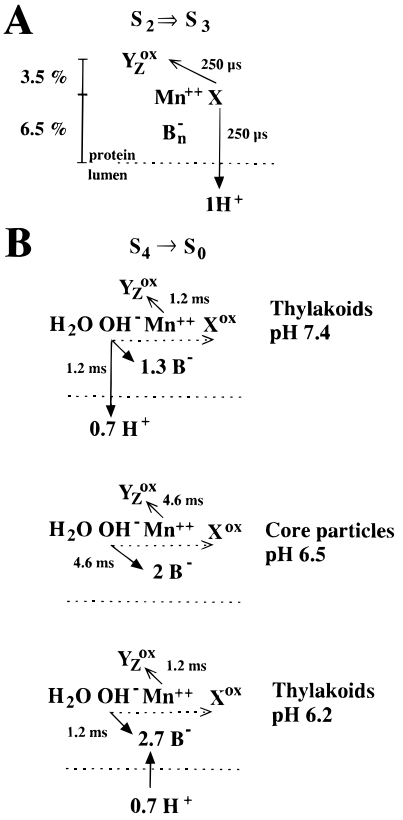

[a] (A) $S_2 \Rightarrow S_3$: X is probably His (Haumann et al., 1996). The electrogenicity of electron transfer (open arrowheads) $X \rightarrow Y_Z^{ox}$ is small ($\leq$ 3.5% of Y_Z^{ox}/Q_A^- formation). The major electrogenic component ($\geq$ 6.5%) is attributed to proton transfer (solid arrowheads) from His^{ox} to the lumen. (B) $S_4 \rightarrow S_0$: The electrogenicity of electron transfer $Mn \rightarrow Y_Z^{ox}$ is small ($\leq$3.5%). The hypothetical transfer of a hydrogen atom to His^{ox} upon its reduction (dashed arrow) is not electrogenic. The variable electrogenicity as observed in thylakoids at pH 6.2 and 7.4 and in core particles at pH 6.5 is attributed to the superimposition of proton transfer (i) from the bound water molecules to the lumen, (ii) to a variable amount of bases (B^-_n) created in the lower transitions, and (iii) from the lumen to remaining bases (for further details see Discussion).

$S_0 \Rightarrow S_1$ (Bögershausen et al., 1996)]. The number of acid groups that contribute to proton release up to S_4 is pH-dependent (Haumann & Junge, 1996). More than three bases are created up to state S_4 at pH 6.1. Consequently, on $S_4 \rightarrow S_0$ not only are the three protons that are produced by the final oxidation of water all swallowed by these previously activated bases but also additional protons are taken up from the lumen. At pH 7.4, on the contrary, the number of preformed bases in S_4 is lower than three so that some of the protons from water are released into the lumen (Haumann & Junge, 1994). Contrastingly, in core particles the ratio between preformed bases and protons from water is balanced, all protons are taken up by these bases, and none is released into the lumen on $S_4 \rightarrow S_0$ (Bögershausen & Junge, 1995).

This reasoning straightforwardly explains the variability of the electrogenicity on transition $S_4 \rightarrow S_0$. We have only to place the peripheral acids about halfway between the OEC and the lumen. This is shown in Scheme 1B: One proton is transfered to X^{ox} upon its reduction. This reaction is supposedly not electrogenic (see next section), and it occurs concomitantly with the following reactions: (i) At pH 7.4 (Scheme 1B, left) the large electrogenicity on $S_4 \rightarrow S_0$ (Table 2) resulted from the transfer of 1.3 protons to preformed bases and the transfer of 0.7 protons into the lumen. (ii) At pH 6.5 in core particles only the two preformed bases are reprotonated. (iii) The smallest electrogenicity that we observed at pH 6.2 in thylakoids likely indicated the transfer of two protons to the preformed bases. It was in part compensated by the further transfer of protons in the reverse direction, from the lumen to these bases.

(4) On the Topology of Redox Cofactors and Protolytic Groups at the Oxidizing Side of PSII. The structure of the OEC and the relative distances between the Mn cluster, the redox cofactor X, and Y_Z are still controversial: Some authors have proposed that the Mn cluster is very close to Y_Z (at about 4.5 Å) on the basis of pulsed EPR data (Gilchrist et al., 1995). Other authors, however, arrived at larger distances ($\geq$15 Å) by also using EPR (Kodera et al., 1995; Hara et al., 1996) and by a molecular modeling approach (Svensson et al., 1996). As a further possibility, the existence of two Mn dimers with a large distance between them has been proposed (Smith & Pace, 1996). We observed that the electrogenicity of electron transfer from Mn to Y_Z^{ox} and probably also from X to Y_Z^{ox} was small ($\leq$ 3.5%). Accordingly, Mn_4, X, and Y_Z are located approximately in the same depth in the membrane. If X is identified with histidine (Haumann et al., 1996), these data are compatible with the notion that His is a ligand to the Mn cluster [see also Tang et al. (1994) and Ahrling and Pace (1995)].

The raw extents of the electrogenic components with the typical rates of electron transfer OEC $\rightarrow Y_Z^{ox}$ ranged over 2.5−13% of the extent attributable to Y_Z^{ox}/Q_A^- formation. The distance between the latter is about 26.5 Å (see above). Thus, the electrogenicities of the reactions at the OEC translated into distances of 0.7−3.5 Å under the assumption of a homogenous dielectric. These distances are very small indeed. The distance of Y_D^{ox} to the boundary has been determined as about 20 Å (Isogai et al., 1990). Y_Z and Y_D are likely placed symmetrically with respect to P_{680} (Koulougliotis et al., 1995). Extending the estimate of the effective dielectric permittivity between P_{680} and Q_A of 10 [Mulkidjanian et al. (1996) and references therein] also to the region between Y_Z and the protein boundary one calculates a distance of 2.7 Å between the latter from the observed electrogenicity on transition $S_2 \Rightarrow S_3$, which is 13%. This figure is only compatible with the above estimate of 20 Å if a unreasonably high dielectric permittivity betweenY_Z and the lumen is assumed, namely, 75, which is about the one of water. Thus, it seems reasonable to consider that the protein/water boundary is closer to Y_Z than to Y_D. Such a location is compatible with the easier reduction of the former by external reductants (Yerkes & Babcock, 1980) and with a more hydrophilic environment of Y_Z as compared with Y_D (Svensson et al., 1991). A value of 20−40 has been estimated for the dielectric permittivity of the Q_B binding site [for review see Shinkarev et al. (1992)]. Assuming the same figure for the dielectric permittivity between Y_Z and the lumen, the latter distance may be recalculated to about 11 Å. This figure compares well with a distance of 10 Å between the bacterial counterpart of Y_Z, Arg135, and the protein boundary in *Rhodopseudomonas viridis* (Deisenhofer et al., 1995). It is further compatible with the estimated extension of PSII into the thylakoid lumen from electron microscopy data (Boekema et al., 1994). We conclude that the extrinsic proteins likely do not contribute to the elec-

Chart 1: Tentative Model of the Arrangement of Cofactors and Bases at the Lumenal Side of PSII[a]

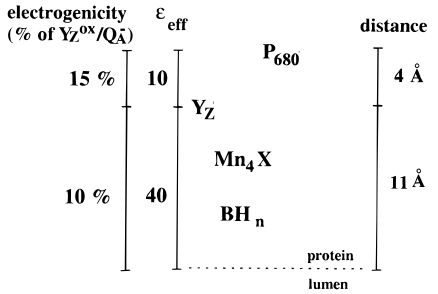

[a] The positioning of Y_Z, Mn_4, and X of the OEC and of the peripheral deprotonable groups BH relative to each other and to the protein boundary was based on a tentative calibration of the extents of the electrogenic components with variable dielectric permittivities (see text for details). The placement of the cofactors is in line with a previous proposal that was based on local electrochromism (Mulkidjanian et al., 1996).

trogenicity of electron and proton transfer at the OEC.

Chart 1 gives a tentative model for the distances between cofactors and the protein/water boundary at the oxidizing side of PSII. This tentative model is based on the above dielectric permittivities (see legend of Scheme 1B), a position of Y_Z similar to LArg135 in the bacterial reaction center (Michel & Deisenhofer, 1988), and the placement of manganese on D1 in the region of D1Asp170 (Pakrasi, 1995) and out of the line that connects Y_Z and P_{680} (Mulkidjanian et al., 1996). The embedding of the peripheral acid groups (BH) more deeply in the protein is further in line with their electrostatically induced deprotonation and their sensing of the charges that are placed on Y_Z^{ox} and the Mn cluster (Lavergne & Junge, 1993; Haumann & Junge, 1996).

CONCLUSIONS

We studied the electrogenicities of electron and proton transfer at the oxidizing side of PSII in liposome-reconstituted PSII core particles by electrometry and in thylakoids by transmembrane electrochromism. The electrogenicity between Y_Z and Q_A served as standard, 100%. Electron transfer from Y_Z to P_{680}^+ produced about 15% electrogenicity. Electron transfer from the Mn_4X entity of the OEC to Y_Z^{ox} was much less electrogenic ($\leq$3.5%). Larger electrogenic components of about 7% were attributed to proton transfer from the oxidized cofactor X to the lumen on transition $S_2 \Rightarrow S_3$ and to the protolytic reactions coupled to the final oxidation of water on transition $S_4 \rightarrow S_0$. A tentative calibration of the observed extents of the electrogenic components resulted in a model for the vertical arrangement of cofactors in the membrane with the following features: (1) The distance between Y_Z and the protein/water boundary is about 11 Å. (2) Mn_4 and X are closely apposed and placed only slightly ($\leq$3.5 Å) below Y_Z. (3) The peripheral deprotonable acid groups are placed about halfway between Mn_4X and the boundary.

ACKNOWLEDGMENT

We thank H. Kenneweg for technical assistance and Dr. H.-W. Trissl and N. Spreckelmeyer for their generous help with the equipment used for electrometry.

REFERENCES

Ahrling, K. A., & Pace, R. J. (1995) *Biophys. J. 68*, 2081−2090.
Allakhverdiev, S. I., Klimov, V. V., & Demeter, S. (1992) *FEBS Lett. 297 (1, 2)*, 51−54.
Barry, B. A. (1993) *Photochem. Photobiol. 57*, 179−188.
Barry, B. A. (1995) *Methods Enzymol. 258*, 303−319.
Barry, B. A., Boerner, R. J., Julio, C., & Paula, d. (1994) *Adv. Photosynth. 1*, 217−257.
Beroza, P., Fredkin, D. R., Okamura, M. Y., & Feher, G. (1995) *Biophys. J. 68*, 2233−2250.
Berthomieu, C., & Boussac, A. (1995) *Biochemistry 34*, 1541−1548.
Boekema, E. J., Boonstra, A. F., Dekker, J. P., & Rögner, M. (1994) *J. Bioenerg. Biomembr. 26*, 17−29.
Bögershausen, O., & Junge, W. (1995) *Biochim. Biophys. Acta 1230*, 177−185.
Bögershausen, O., Haumann, M., & Junge, W. (1996) *Ber. Bunsenges. Phys. Chem. 100* (12), 1987−1992.
Boussac, A., Zimmermann, J. L., Rutherford, A. W., & Lavergne, J. (1990) *Nature 347*, 303−306.
Brettel, K., Schlodder, E., & Witt, H. T. (1984) *Biochim. Biophys. Acta 766*, 403−415.
Britt, R. D. (1996) in *Oxygenic photosynthesis: The light reactions* (Ort, D., & Yocum, C. F., Eds.) pp 137−164, Kluwer, Dordrecht, The Netherlands.
Brudvig, G. W. (1995) *Adv. Chem. Ser. 246*, 249−263.
Cherepanov, D. A., Haumann, M., Junge, W., & Mulkidjanian, A. (1995) in *Photosynthesis: from light to biosphere I* (Mathis, P., Ed.) pp 531−535, Kluwer, Dordrecht, The Netherlands.
Conjeaud, H., & Mathis, P. (1980) *Biochim. Biophys. Acta 590*, 353−359.
Debus, R. J. (1992) *Biochim. Biophys. Acta 1102*, 269−352.
Deisenhofer, J., Sinning, I., & Michel, H. (1995) *J. Mol. Biol. 246*, 429−457.
Diner, B. A., & Babcock, G. T. (1996) in *Oxygenic photosynthesis: the light reactions* (Ort, D. R., & Yocum, C. F., Eds.), pp 213−247, Kluwer, Dordrecht, The Netherlands.
Diner, B. A., & Nixon, P. J. (1992) *Biochim. Biophys. Acta 1101*, 134−138.
Drachev, L. A., Kaule, A. D., Semenov, A. Y., Severina, I. I., & Skulachev, V. P. (1979) *Anal. Biochem.* 96, 250−262.
Drachev, L. A., Semenov, A. Y., Skulachev, V. P., Smirnova, I. A., Chamorovsky, S. K., Kononenko, A. A., Rubin, A. B., & Aspenskaya, N. Y. (1981) *Eur. J. Biochem. 117*, 483−489.
Dracheva, S. M., Drachev, I. A., Konstantinov, A. A., Semenov, A. Y., Skulachev, V. P., Arutyunyan, A. M., Shuvalov, V. A., & Zaberezhnaya, S. M. (1987) *Biol. Membr. 4*, 1269−1288.
Förster, V., & Junge, W. (1985) *Photochem. Photobiol. 41*, 183−190.
Ford, R. C., Rosenberg, M. F., Shepherd, F. H., McPhie, P., & Holzenburg, A. (1995) *Micron 26*, 133−140.
Gilchrist, M. L., Ball, J. A., Randall, D. W., & Britt, R. D. (1995) *Proc. Natl. Acad. Sci. U.S.A. 92*, 9545−9549.
Hara, H., Kawamori, A., Astashkin, A. V., & Ono, T. (1996) *Biochim. Biophys. Acta 1276*, 140−146.
Haumann, M., & Junge, W. (1994) *Biochemistry 33*, 864−872.
Haumann, M., & Junge, W. (1996) in *Advances in Photosynthesis: Oxygenic Photosynthesis—The Light Reactions* (Ort, D., & Yocum, C. F., Eds.) pp 165−192, Kluwer, Dordrecht, The Netherlands.
Haumann, M., Bögershausen, O., & Junge, W. (1994) *FEBS Lett. 355*, 101−105.
Haumann, M., Hundelt, M., Drevenstedt, W., & Junge, W. (1995) in *Photosynthesis: from Light to Biosphere* (Mathis, P., Ed.) pp 333−336, Kluwer, Dordrecht, The Netherlands.
Haumann, M., Drevenstedt, W., Hundelt, M., & Junge, W. (1996) *Biochim. Biophys. Acta 1273*, 237−250.
Haumann, M., Bögershausen, O., Cherepanov, D. A., Ahlbrink, R., & Junge, W. (1997), *Photosynth. Res.* (in press).
Hook, F., & Brzezinski, P. (1994) *Biophys. J. 66*, 2066−2072.
Hundelt, M., Haumann, M., & Junge, W. (1997) *Biochim. Biophys. Acta* (in press).
Isogai, Y., Itoh, S., & Nishimura, M. (1990) *Biochim. Biophys. Acta 1017*, 204−208.
Jahns, P., Lavergne, J., Rappaport, F., & Junge, W. (1991) *Biochim. Biophys. Acta 1057*, 313−319.
Junge, W. (1976) in *Chemistry and Biochemistry of Plant Pigments* (Goodwin, T. W., Ed.) pp 233−333, Academic Press, London.

Junge, W., & Witt, H. T. (1968) *Z. Naturforsch. 23b*, 244−254.
Klein, M. P., Sauer, K., & Yachandra, V. K. (1993) *Photosynth. Res. 38*, 265−277.
Kodera, Y., Hara, H., Astashkin, A. V., Kawamori, A., & Ono, T. (1995) *Biochim. Biophys. Acta 1232*, 43−51.
Koulougliotis, D., Tang, X. S., Diner, B. A., & Brudvig, G. W. (1995) *Biochemistry 34*, 2850−2856.
Lavergne, J., & Junge, W. (1993) *Photosynth. Res. 38*, 279−296.
Lavergne, J., & Leci, E. (1993) *Photosynth. Res. 35*, 323−343.
Mamedov, M. D., Beshta, O. E., Samuilov, V. D., & Semenov, A. Y. (1994) *FEBS Lett. 350*, 96−98.
Mamedov, M. D., Lovyagina, E. R., Verkhovskii, M. I., Semenov, A. Y., Cherepanov, D.A., & Shinkarev, V. P. (1995) *Biochemistry (Moscow) 59*, 327−341.
Michel, H., & Deisenhofer, J. (1988) *Biochemistry 27* (1), 1−7.
Mulkidjanian, A. Y., Cherepanov, D. A., Haumann, M., & Junge, W. (1996) *Biochemistry 35*, 3093−3107.
Noguchi, T., Inoue, Y., & Satoh, K. (1993) *Biochemistry* 32, 7186−7195.
Ono, T., & Inoue, Y. (1991) *FEBS Lett. 278* (2), 183−186.
Pakrasi, H. B. (1995) *Annu. Rev. Genet. 29*, 755−776.
Pakrasi, H. B., & Vermaas, W. F. J. (1992) in *The Photosystems: Structure, Function and Molecular Biology* (Barber, J., Ed.) pp 231−257, Elsevier Science Publishers, Dordrecht, The Netherlands.
Pokorny, A., Wulf, K., & Trissl, H. W. (1994) *Biochim. Biophys. Acta 1184*, 65−70.
Rappaport, F., Porter, G., Barber, J., Klug, D. R., & Lavergne, J. (1995) in *Photosynthesis: from light to biosphere II* (Mathis, P., Ed.) pp 345−350, Kluwer, Dordrecht, The Netherlands.
Renger, G. (1979) *Biochim. Biophys. Acta 547*, 103−116.
Renger, G., & Hanssum, B. (1992) *FEBS Lett. 299*, 28−32.
Ruffle, S. V., Donnelly, D., Blundell, T. L., & Nugent, J. H. A. (1992) *Photosynth. Res. 34*, 287−300.
Schaffernicht, H., & Junge, W. (1982) *Photochem. Photobiol. 36*, 111−115.
Schliephake, W., Junge, W., & Witt, H. T. (1968) *Z. Naturforsch. 23*, 1571−1578.
Schlodder, E., Brettel, K., & Witt, H. T. (1985) *Biochim. Biophys. Acta 808*, 123−131.
Schönknecht, G., Althoff, G., & Junge, W. (1990) *FEBS Lett. 277*, 65−68.
Schönknecht, G., Althoff, G., & Junge, W. (1992) *J. Membr. Biol. 126*, 265−275.
Shinkarev, V. P., Takahashi, E., & Wraight, C. A. (1992) in *The photosynthetic bacterial reaction center* (Breton, J., & Vermeglio, A., Eds.) pp 375−387, Plenum Press, New York.
Smith, P. J., & Pace, R. J. (1996) *Biochim. Biophys. Acta 1275*, 213−220.
Styring, S., Davidsson, L., Tommos, C., Vermaas, W. F. J., Vass, I., & Svensson, B. (1993) *Photosynthetica 28*, 225−241.
Svensson, B., Vass, I., & Styring, S. (1991) *Z. Naturforsch.* 46, 765−776.
Svensson, B., Etchebest, C., Tuffery, P., van Kan, P., Smith, J., & Styring, S. (1996) *Biochemistry* 35, 14486−14502.
Tang, X. S., Diner, B. A., Larsen, B. S., Gilchrist, M. L., Lorigan, G. A., & Britt, R. D. (1994) *Proc. Natl. Acad. Sci. U.S.A. 91*, 704−708.
Tang, X. S., Randall, D. W., Force, D. A., Diner, B. A., & Britt, R. D. (1996) *J. Am. Chem. Soc. 118* (32), 7638−7649.
Trissl, H. W. (1989) *FEBS Lett. 244*, 85−88.
Trissl, H. W., & Gräber, P. (1980) *Bioelectrochem. Bioenerg. 7*, 167−186.
Un, S., Brill, T. M., & Zimmermann, J. L. (1994) *Proc. Natl. Acad. Sci. U.S.A. 91*, 5262−5266.
van Leeuwen, P. J., Nieveen, M. C., van de Meent, E. J., Dekker, J. P., & Van Gorkom, H. J. (1991) *Photosynth. Res. 28*, 149−153.
van Leeuwen, P. J., Heimann, C., Kleinherenbrink, F. A. M., & Van Gorkom, H. J. (1992) in *Research in photosynthesis* (Murata, N., Ed.) pp 341−344, Kluwer, Dordrecht, The Netherlands.
van Leeuwen, P. J., Heimann, C., Gast, P., Dekker, J. P., & Van Gorkom, H. J. (1993) *Photosynth. Res. 38*, 169−176.
van Mieghem, F. J. E., Satoh, K., & Rutherford, A. W. (1991) Biochim. Biophys. Acta 1058, 379−385.
Vermaas, W. F. J., Styring, S., Schröder, W. P., & Andersson, B. (1993) *Photosynth. Res. 38*, 249−263.
Vos, M. H., Van Gorkom, H. J., & van Leeuwen, P. J. (1991) *Biochim. Biophys. Acta 1056*, 27−39.
Yerkes, C. T., & Babcock, G. T. (1980) *Biochim. Biophys. Acta 590*, 360−372.
Yerkes, C. T., Babcock, G. T., & Crofts, A. R. (1983) *FEBS Lett. 158* (2), 359−363.

BI963114P